Available online at www.sciencedirect.com

ScienceDirect

Procedia Materials Science 5 (2014) 408 – 415

Procedia Materials Science

www.elsevier.com/locate/procedia

International Conference on Advances in Manufacturing and Materials Engineering, AMME 2014

Microstructure evolution during fusion welding of rheocast AA7075 alloy

S.Sandhya[a], R.Mahemaa[b], G.Phanikumar[a,*]

[a] *Department of Metallurgical and Materials Engineering, Indian Institute of Technology Madras, Chennai - 600036, Tamilnadu, India*
[b] *Department of Metallurgical and Materials Engineering, National Institute of Technology Trichy, Tiruchirapalli - 620015, Tamilnadu, India*

Abstract

The microstructural evolution during varying thermal gradients of rheocast AA7075 aluminium alloy was investigated. To perform this study, semi-solid billets of non-dendritic microstructure were produced using Linear Electro Magnetic Stirrer (LEMS). Gas Tungsten arc welding (GTAW) was conducted to simulate varying thermal gradients near fusion zone. Welding simulations were performed using SYSWELD®. Quantitative metallography was used to aid the analysis. Numerical simulations and quantitative results show that the width of the partially melted zone (PMZ) plays a vital role in the nucleation mechanism and dendritic microstructure formation in this class of alloys.

Selection and peer-review under responsibility of Organizing Committee of AMME 2014

Keywords: Semi-solid processing; Thermal gradient; Partially melted zone; Globular; Dendritic; SYSWELD®

1. Introduction

AA 7075 wrought aluminum alloys are extensively used in aerospace industry due their light weight and high specific strength to weight ratio. Generally, wrought alloys are hot and/or cold worked mechanically, to achieve dense parts with higher strength. However, few of them are processed through casting routes without casting flaws. Semi-solid processed alloys is a class of that lies between wrought (dilute alloys) and cast (near eutectic) alloys. In these alloys, the alloy in the mushy state is subjected to vigorous stirring during solidification. Strong convective forces shear the liquid metal and increase mobility of solute in the liquid to alter the dendritic

* Corresponding author. Tel.:+91-44-2257-4770.
E-mail address: gphani@iitm.ac.in

Selection and peer-review under responsibility of Organizing Committee of AMME 2014
doi:10.1016/j.mspro.2014.07.283

morphology of the solid into globular/spherical microstructure [Flemings (1974)]. It also addresses some of the deficiencies of conventional casting process by producing low porosities or porosity free castings, which improves weldability of semi-solid formed components [Govender et al. (2007)].

This work is motivated by the need to study weldability of any alloy class that needs to mature towards fabrication of complex parts. Semi-solid processing has emerged as a route to produce alloys that are otherwise not readily diecastable. Large freezing range alloys could be produced with globular microstructure using semi-solid processing (SSP), so that they could be easily die-cast in semi-solid state. Similarly, wrought alloys which face solidification cracking or hot cracking issues could be made diecastable by modifying the microstructure as globular. With the semisolid processed & globular microstructure emerging as a new class of materials, it is important to probe weldability of these alloys as welding is an important fabrication technique to produce complex parts from individual parts. In this study, we explore the role of thermal gradient near the fusion boundary on the microstructure formation in the weldment of rheocasted wrought aluminium 7075 alloy.

Nomenclature

G_T	Thermal Gradient
W_P	Width of partially melted zone
h	Convective heat transfer co-efficient
A	Area of primary α-Al
P	Perimeter of primary α-Al

2. Experiment procedure

7075 aluminium alloy was semi-solid processed by rheocasting in a graphite mould placed inside Linear Electro Magnetic Stirrer (LEMS) [Kumar (2008)]. Cast plates of thickness 8 mm were machined from the billets. Bead on plate autogenous GTAW was performed. To simulate varying thermal gradients near fusion zone, GTAW experiments were performed by providing copper backing plate with and without water cooling condition at the bottom of weld coupons. Transverse cross-section of the samples were taken at the centre of the weld to examine the weld profile and microstructure in the fusion zone. To characterize the metallography, initially the surface of the samples were well polished using various grades of emery paper followed by diamond polishing. Then they were etched by Keller's reagent containing 2.5 % HNO_3, 1.5 % HCl, 0.5 % HF and remaining H_2O for optical microscopy. Quantitative metallography provided shape factor as measure of globularity of primary α-Al grains using the equation $(4\pi A)/P^2$, where the cross sectional area is (A) and perimeter is (P) of the primary α-Al grains are determined using image processing.

3. Numerical simulation

Finite element method (FEM) has matured with increase in the number of commercially available codes that make use of computational power and quickly provide realistic simulations of computational welding mechanics to aid in the understanding of the role of thermal, mechanical and material properties on welding. A 3-D model of the semisolid cast plate was created with visual weld pre-processor using eight node cube elements, in order to understand the weld pool geometry and thermal distribution influenced by heat transfer. The finite element mesh shown in Fig. 1 is modelled with adaptive meshing. The thermal gradient near the FZ and PMZ are high hence, mesh with finer elements are modelled along these zones in order to have better aspect ratio. Beyond the weld zones the gradient is less and so mesh with coarser elements are made to reduce the computational time. Pentagonal elements shown in Fig. 2 are used to have smooth transition between higher (finer mesh) and lower (coarser mesh) thermal gradients. Temperature dependent material properties such as thermal conductivity and specific heat as a function of temperature as specified in the literature [Feulvarch et al. (2006)] are given as input parameters to the 3-D model.

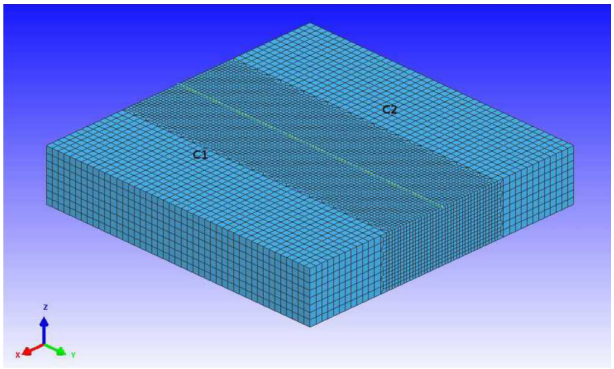

Fig. 1. 3-D mesh of semi-solid cast plate

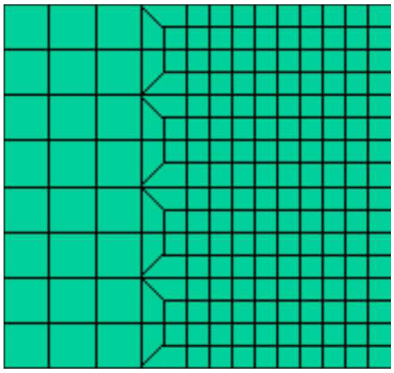

Fig. 2. Mesh in transition region

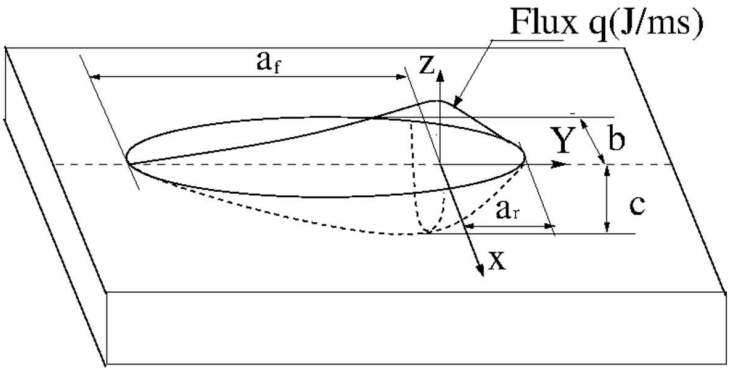

Fig: 3. Goldak double ellipsoidal heat source model

3.1. Heat source fitting tool

Heat source fitting (HSF) tool is a facility available within the SYSWELD® software, which enables the user to calibrate the heat source parameters to perform transient thermal analysis of welding [Bate et al. (2009)]. Several heat source models from simple point sources of Rosenthal to complex Goldak double ellipsoidal Gaussian distribution are available. The more complex the heat distributions, the more accurate the fit of the thermal profiles. Since this analysis is concerned with TIG welding, a pre-defined double ellipsoidal heat source model defined by Goldak and co-workers was selected [Goldak et al. (1984); Bate et al. (2009)]. The calibration of heat source parameters was achieved by a combination of two methods. Firstly, a temperature contour plot showing different regions of the weld zone was taken and compared with the metallographic cross-sections of weld profile taken using low magnification stereo microscopy. Secondly, time-temperature plot of HSF tool was compared to the thermocouple readings taken during experimentation.

In this model the front half is the quadrant of one ellipsoidal heat source and the rear half is the quadrant of another ellipsoidal heat source. In order to reduce the computation time in the transient analysis, a moving reference frame (x,ξ,z) attached with the heat source is used instead of a stationary reference frame (*x,y,z*). SYSWELD uses the following Eq . 1, Eq . 2 & Eqn. 3, to define the power density distribution inside front and rear regions of the heat source respectively [Goldak et al. (1984)].

$$q_f(x,\xi,z,t) = \frac{6\sqrt{3}\,Q_f}{a_f bc\pi\sqrt{\pi}} . e^{-3x^2/a_f{}^2} . e^{-3\xi^2/b^2} . e^{-3z^2/c^2} \quad (1)$$

$$q_r(x,\xi,z,t) = \frac{6\sqrt{3}\,Q_r}{a_r bc\pi\sqrt{\pi}} . e^{-3x^2/a_r{}^2} . e^{-3\xi^2/b^2} . e^{-3z^2/c^2} \quad (2)$$

$$\xi = \mathrm{y} - \mathrm{v}(\tau - \mathrm{t}) \quad (3)$$

Physically, these parameters are radial dimensions of the molten zone namely front length (a_f), rear length (a_r), width of molten zone (b) and depth of molten zone (c). Q_f and Q_r are the front and rear heat source intensity parameters respectively is the welding velocity and τ is the lag factor defining the position of heat source at time t=0. The heat source parameters are adjusted in an iterative manner to achieve best fit.

4. Results and Discussions

The microstructure of as received Al 7075 alloy exhibits long dendritic microstructure (Fig. 4). Upon semi-solid processing using LEMS, the dendrites get fragmented and transformed to non-dendritic primary α-Al grains surrounded by a low melting secondary phase (Fig. 5). Typical transverse cross-section of the weld profile shows various zones namely base material, partially melted zone and fusion zone. Fusion zone is the region which is completely melted during welding. Partially melted zone is the region adjacent to the fusion zone, and the width of this zone plays a major role for globular microstructure formation in the fusion zone of the semi-solid processed alloys. Depending on the thermal gradient along the fusion boundary, width of the partially melted zone varies which is related by $G_T = (T_L - T_E)/W_P$. When the thermal gradient is less the width of PMZ is more, hence more heterogeneous nucleation sites as that of base material favours the globular microstructure formation in fusion zone. The detailed description of the nucleation mechanism occurring in the PMZ of the semi-solid processed alloy are discussed in detail elsewhere [Sandhya and Phanikumar (2013)].

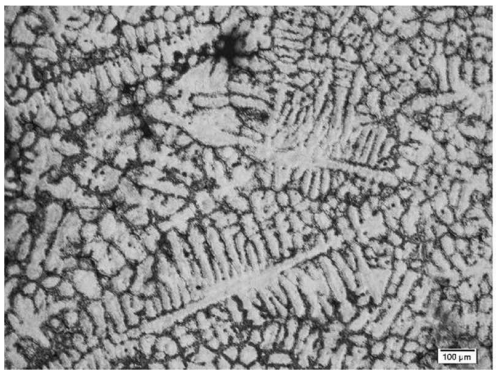

Fig. 4. Microstructure of as received Al 7075

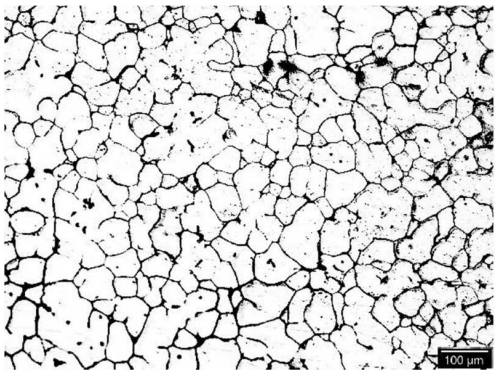

Fig. 5. Microstructure of semi-solid processed Al 7075

Fig. 6, Fig. 7 and Fig. 8 shows the comparison between measured and calculated weld geometry and thermal cycle for the TIG welds in as welded, copper backing and both copper backing and water cooling conditions respectively. In the figures the region marked as FZ is the fusion zone above liquidus temperature (T_L) and the region marked as PMZ is the partially melted zone above secondary phase melting temperature (T_E).

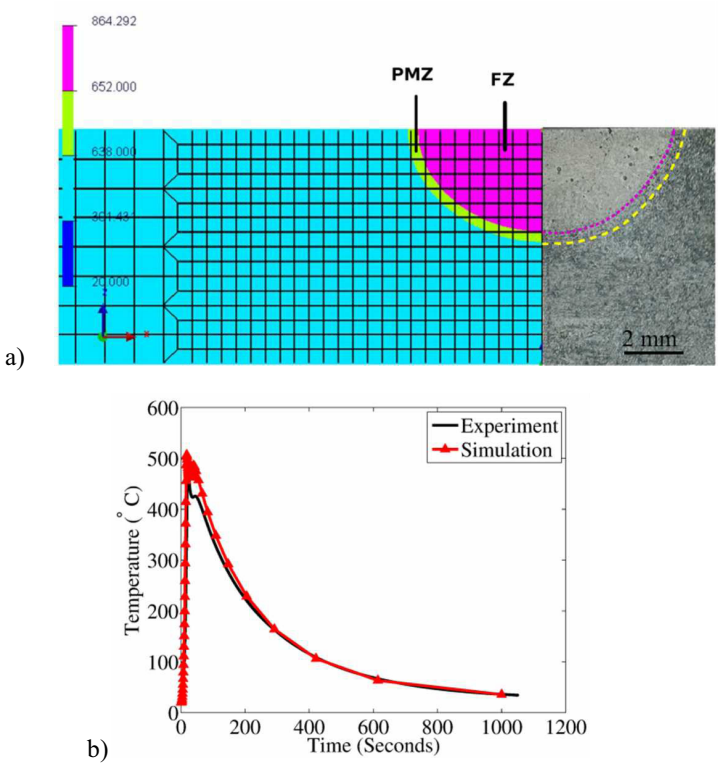

Fig: 6. (a) Thermal profile and (b) Thermal cycle of TIG welded SSP AA 7075 in as welded conditions

Table 1. Results of thermal gradient and width of PMZ of AA 7075 TIG welded with different cooling conditions

Welding conditions	G_T (*K/mm*)	Width of PMZ (*mm*)
As weld	44	0.315
Copper backing	80	0.1
Copper backing and water cooling	100	0.05

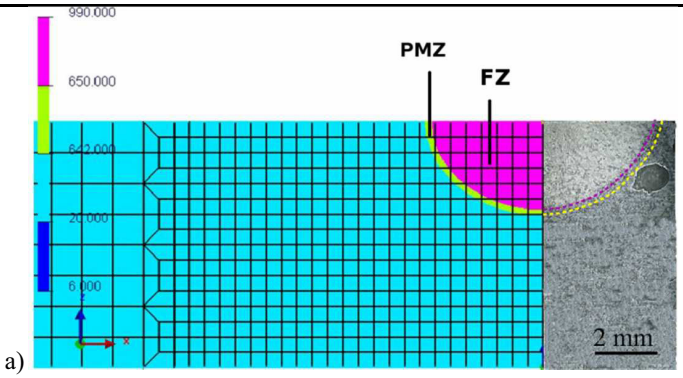

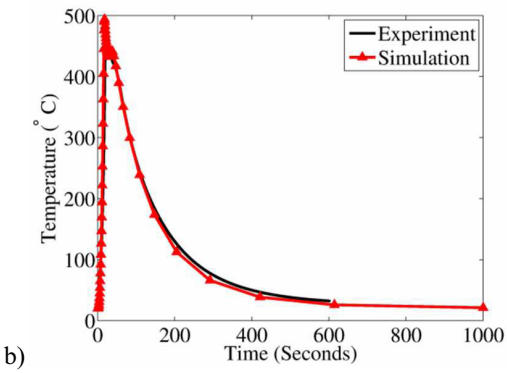

b)

Fig: 7. (a) Thermal profile and (b) Thermal cycle of TIG welded SSP AA 7075 with copper backing conditions

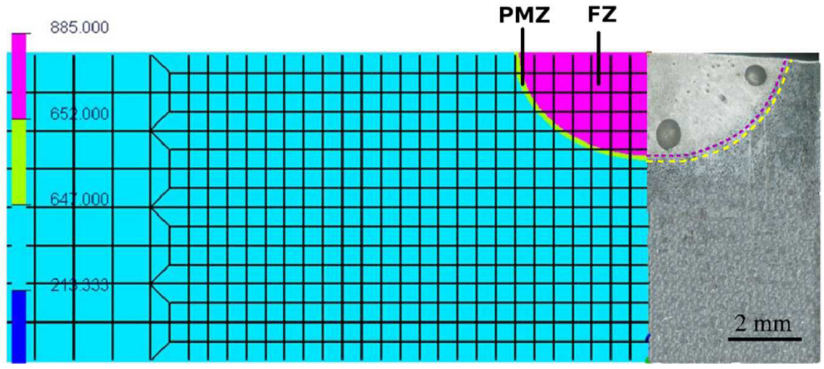

a)

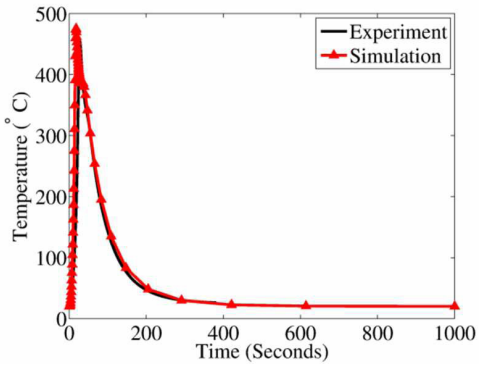

b)

Fig: 8. (a) Thermal profile and (b) Thermal cycle of TIG welded SSP AA 7075 with copper backing and water cooling conditions

The convective heat loss is predicted with a heat transfer coefficient value [Preston et al. (2003)] i.e., for air cooling $h=35\ Wm^{-2}\ K^{-1}$, copper backing plate $h=\ Wm^{-2}\ K^{-1}$ and for both copper backing and water cooling $h=350\ Wm^{-2}\ K^{-1}$ are specified on the boundary surface to achieve best fit between thermal cycle and weld profiles. Numerically measured thermal gradient and the width of PMZ under different welding conditions are listed in Table.1. In all the cases, the width of PMZ is very small hence, fewer nucleation sites as that of base material advect into the fusion zone providing more free growth for dendritic morphology. This is confirmed by observing the microstructure at the base material - FZ interface (Fig. 9), where long dendritic morphology grow towards the center of the fusion zone from the fusion boundary. From the histogram (Fig. 10(a)) the microstructure of semi-solid processed Al 7075 alloy

has a shape factor value closer to that of rosette morphology, whereas for the TIG welded samples (Fig. 10(b) - Fig. 10(d)) the shape factor value approaches zero i.e. dendritic microstructure.

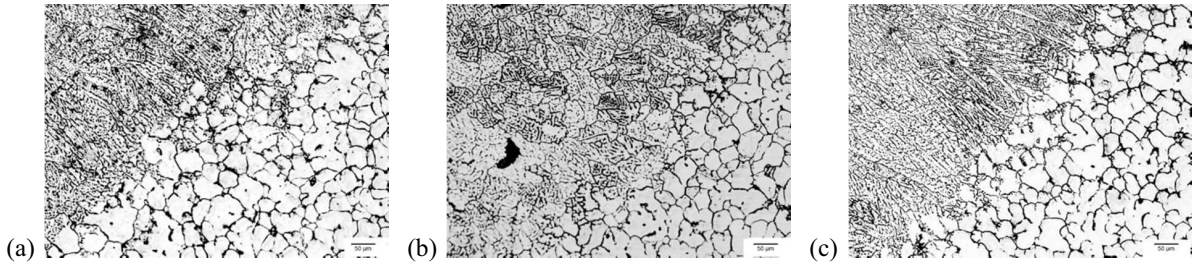

Fig. 9. Optical micrographs in the PMZ-FZ interface of AA 7075 under (a) as welding (b) copper backing (c) copper backing and water cooling conditions

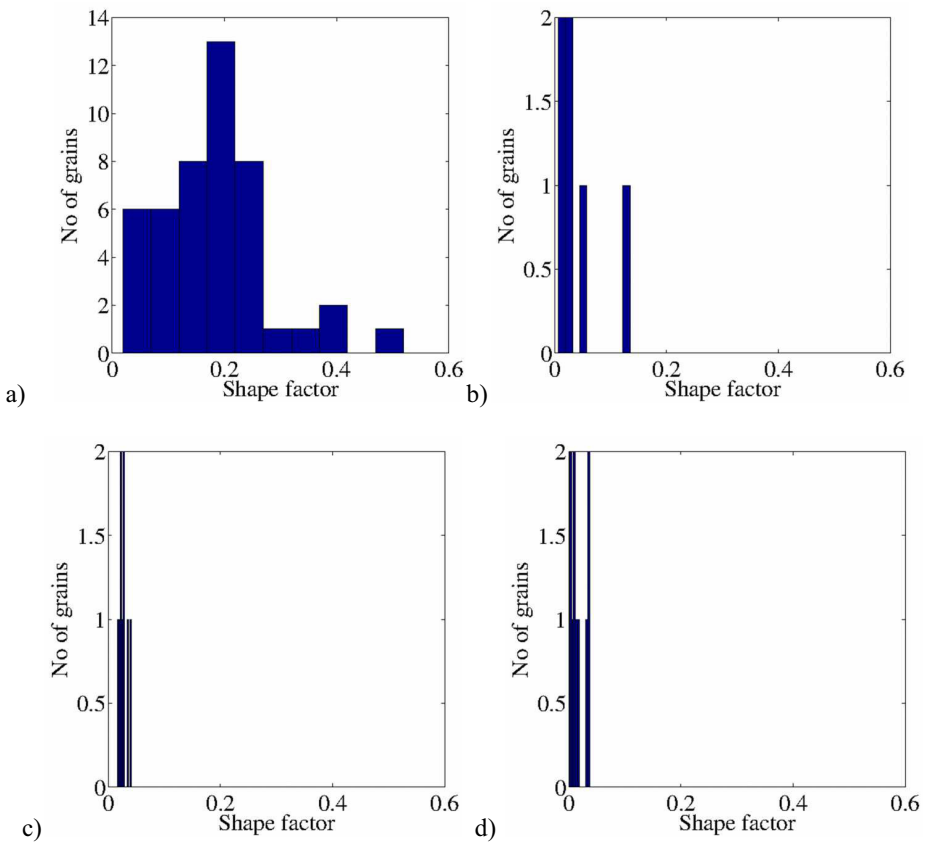

Fig. 10. Histogram showing shape factor distribution in (a) base metal (b) FZ of weld without additional cooling at bottom surface (c) FZ of weld with Cu backing (d) FZ of weld with Cu backing & water cooling

The microstructure study shows that the fusion zone of a fusion weld between two semi-solid processed plates of globular microstructure deviates from the globular microstructure when the width of the partially melted zone is small. This is in corroboration with the study presented earlier [Sandhya and Phanikumar (2013)] where a wider partially melted zone led to globular microstructure in the fusion zone. The width of partially melted zone plays an

important role in determining the microstructure of the fusion zone of welds between semi-solid processed samples of globular microstructure.

5. Conclusions

1. Semi-solid processing can be effectively carried out using Linear Electro Magnetic Stirring on low freezing range Al 7075 alloy.
2. Numerical results conclude that thermal gradient along the fusion boundary influences the width of partially melted zone, which in turn governs the nucleation mechanism occurring in the fusion zone.
3. The low freezing range in this class of alloy is the major reason for smaller W_P; hence the solidification morphology changes from globular to dendritic morphology.

6. Acknowledgements

The authors would like to thank Prof. Pradip Dutta, Ms.Hamsalakshmi and the National Semi Solid Forming Facility, IISc Bangalore for providing the semisolid billets for this study; Prof. N. Siva Prasad and Mr. Kala Shirish, Department of Mechanical Engineering, IIT Madras for providing and helping with SYSWELD® software.

References

Bate, S., Charles, R., Warren, A., 2009. Finite element analysis of a single bead-on-plate specimen using SYSWELD. International Journal of Pressure Vessels and Piping 86, 73 – 78.

Feulvarch, E., Gooroochurn, Y., Boitout, F., Bergheau, J., David, S., DebRoy, T., Lippold, J., Smartt, H., Vitek, J., 2006. 3D modelling of thermofluid flow in friction stir welding. Trends in Welding Research, Proceedings , 261–266.

Flemings, M., 1974. Solidification processing. Metallurgical Transactions 5.

Goldak, J., Chakravarti, A., Bibby, M., 1984. A new finite element model for welding heat sources. Metallurgical Transactions B 15B, 299–305.

Govender, G., Ivanchev, L., Hope, D., Burger, H., Kunene, G., 2007. Comparative study on laser welding and TIG welding of semi-solid high pressure die cast A356 aluminium alloy , pp 1–7.

Kumar, P., 2008. Experimental investigation of Rheocasting using Linear electromagnetic stirring. Ph.D. thesis. Indian Institute of Science, Bangalore, India.

Preston, R.V., Shercliff, H.R., Withers, P.J., Smith, S.D., 2003. Finite element modelling of tungsten inert gas welding of aluminium alloy 2024. Science and Technology of Welding & Joining 8, 10–18.

Sandhya, S., Phanikumar, G., 2013. Investigation of fusion weldments of semi-solid aluminium a356 alloy: Pool geometry and microstructure, Materials Science Forum 765, 751 – 755.